Modeling Heart Pacemaker Tissue by a Network of Stochastic Oscillatory Cellular Automata

Danuta Makowiec

Institute of Theoretical Physics and Astrophysics, University of Gdańsk, Poland
fizdm@univ.gda.pl
http://www.strony.fizdm.ug.edu.pl/ME/

Abstract. Computations performed by a system of cyclic cellular automata, designed to model the principal organization rules known for the tissue of the first cardiac pacemaker — the sinus node, are investigated in terms of Kuramoto order parameters of synchronization. We show that such description provides consistent quantification of stationary states in the model. Finally, the model is used to give possible explanations for changes observed in the sinus node rhythmicity caused by age.

Keywords: cellular automata, synchronization, multiscale modeling.

1 Introduction

Discoveries appearing day by day from biochemical and physiological labs are challenging for computational methods because they need novel conceptions for computation. The natural computations are different from methods to which we got used to in many aspects. It is even said that specifying the problem is demanding [1].

The natural computations are parallel. The natural systems are space distributed, constituted from many different subsystems. The computations are run in parallel in all parts of these systems. The natural computations are dynamical. The present state of each system unit: organizing (as a protein or cell, for example) or functional unit (like a tissue or organ), are recorded in its environment by initiating a sequence, often a cascade, of biochemical processes. Effects of these processes are read back by the same unit to modify, adapt its next state. Since the effects of states are emitted to the environment, the results are dynamically used by other neighboring units. The natural computations are multi-layered. The local environment of any unit consists of elements of other computational systems. They can be different from each other because of, for example, the way of communication. One system passes the information via diffusion of transmitters (neuronal systems) while the other by cell-to-cell direct injection of ions (cardiac cells). So they act at different time and space scales. But these different computational systems penetrate tightly one another providing the robust solution.

In the following we will observe computations performed by a system made of cyclic cellular automata, designed to model the principal organization known for

G. Mauri et al. (Eds.): UCNC 2013, LNCS 7956, pp. 138–149, 2013.

the tissue of the sinus node — the first cardiac pacemaker [2–8]. By computations in this system we understand emerging of the collective state — synchronization of oscillations of individual cells to produce the strong pacemaker signal. To achieve such computational system, the network of coupled discrete-state units is proposed. The elementary units — the basic layer of computations, reveal the electrochemical properties of pacemaker cells. The network of intercell connections establishes the next layer. The sparsity and stochastic heterogeneity, known organizing principles of the pacemaker tissue structure, are taken into account. The adaptive and/or controlling layer is introduced in the so-called tonic way. The regulatory role of the autonomic nervous system is revealed by parameters describing sensitivity of cells for external stimulation.

The model has its roots in Greenberg-Hastings cellular automata modeling the excitable medium[9, 10]. Discrete modeling has become attractive because it provides the opportunity to adjust both assumptions and results in models with natural cellular automata where the natural computations are performed. By natural cellular automata we mean the technics of in vitro models where cultured cardiac cells are placed on special matrices in order to observe emergence and development of cell-to-cell interactions [11, 12].

Therefore, the basic objective of our modeling is to provide a tool which is enable to test intuitions about general mechanisms responsible for the multiscale effects. The work is a continuation of our investigations [13, 14]. In the following the model is rewritten in a compact way, Sec. 2. Then results are presented which were obtained in simulations aimed on effects of heterogeneity among intercellular connections on collective properties of stationary states, Sec.3. The results are expressed in terms of Kuramoto order parameters — the popular tools for quantifying the synchrony among coupled oscillators [19, 20]. We show that such description consistently quantifies collective properties in the studied systems. In last Section we discuss the model properties in order to explain some changes in the sinus node with age.

2 From Natural Computation to Computer Computation

The heart automaticity is originated in the sinoatrial node — a flat tissue located on the right atrium. The node produces sustained oscillations of electrochemical signals. These signals initiate the sequence of events which eventually lead to the whole heart contraction. It is commonly believed that the source of sinoatrial node function is closely related to electrophysiology of each individual cell.

2.1 The Model of a Cell

Physiology of a Pacemaker Cell. There is a sequence of biochemical processes which change the electrical potential of a myocyte — the cardiac cell, membrane. The phenomenon of ions transmission through the membrane the cell: inward (potassium K^+) and outward (sodium Na^+ and calcium Ca^{2+}), is called the action potential. The time interval when the myocyte membrane is

depolarized takes about 400ms what is the half of the time interval between subsequent heart contractions, approximately. In the case of pacemaker cells, the course of the action potential is substantially different from other myocardium cells. The depolarization process is slow, see Fig.1, because the increase in the membrane potential is not caused by sodium Na^+ ions but by calcium Ca^{2+} ions only. Furthermore, after completing the action potential, the membrane potential does not stay resting but rises continuously due to activity of $\mathbf{i_f}$ current and calcium current $\mathbf{i_{Ca(T)}}$, and reaches the threshold value. Then the next action potential develops due to $\mathbf{i_{Ca(L)}}$[2, 3]. The dotted lines in Fig.1 divide the oscillation interval into three physiologically justified stages: 0, 3 and 4, called in the following: *firing*, *refractory* and *activity*, respectively.

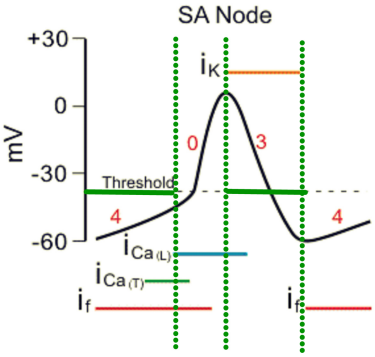

Fig. 1. Membrane potential of a nodal cell in time together with basic currents: $\mathbf{i_f}$, $\mathbf{i_{Ca(T)}}$, $\mathbf{i_{Ca(L)}}$, $\mathbf{i_K}$ that drive the membrane potential change. Diagram is a modified scheme from [3].

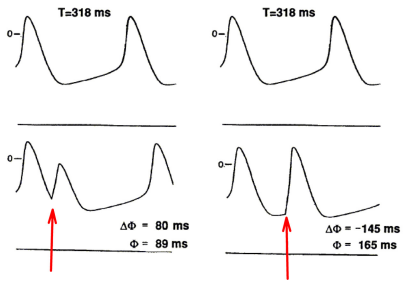

Fig. 2. The effects of depolarizing of pulses (denoted as red arrows) on the spontaneous cycle of a single enzymatically dissociated pacemeker cell from the sinoatrial node of the rabbit. Diagram is a modified scheme from [16, 2]

The, so-called, phase sensitivity [15, 16, 2] describes an important aspect of the pacemaker cell elecrophysiology, see Fig.2. Experiments with rabbit and other mammalian heart cells showed that an external stimulus can influence the intrinsic cycle. It could shorten the cycle if it arrives when a cell is after completing of the action potential, so after stage 3. The perturbation could elongate the period if it comes when the action potential process has not been completed, so during stage 3. In Fig.2 upper plots describe unperturbed membrane potential with the mean period (T) =318 msec. Lower plots show the membrane potential when the pulse appears before the end of the repolarization process, and when the pulse comes later.

Assumptions. We propose to consider an automaton, called *FRA-cell*, to model the sequence of nodal cell cycle. The model is based on the following assumptions:

(i) The cell cycle consists of three successive stages along which the cell progresses: *firing*, *refractory* and *activity*. Upon completion of *activity* stage, the cell immediately enters a new cycle in *firing* stage.
(ii) Each stage is characterized by its maximal duration which is represented by consecutive stage states. The number of states for each stage is fixed. As soon as the duration of a given stage is reached, the transition to the first state of next stage of the cell cycle occurs.
(iii) The time at which the transition takes place can vary in a random manner.
(iv) If a cell is in *activity* stage and receives a stimulus then it switches to *firing* stage.
(v) If a cell is in *refractory* stage and receives a stimulus then it stays longer in this stage.

The *FRA*-Cell Model

(a) Let $\Sigma = \{F_i, R_j, A_k\}$ be the state space of a FRA-cell, $i, j, k \in \{1, 2, \ldots, n_\sigma\}$, with $n_\sigma \in \{f, r, a\}$ denoting the duration of stages *firing*, *refractory*, and *activity*, respectively.
Let $\phi(t) = \sigma_l$ is the phase of a FRA cell at time t, $\sigma_l \in \Sigma$.
(b) The cellular phase in the next time step $\phi(t+1)$ is

$$\begin{aligned} \phi(t+1) &= \text{next}(\sigma)_1, \qquad \text{with probability} \quad \left(\frac{l}{n_\sigma}\right)^\xi \quad \text{with} \quad l \le n_\sigma, \\ \phi(t+1) \quad &= \sigma_{l+1}, \qquad \text{otherwise} \end{aligned} \tag{1}$$

where next(*firing*)=*refractory*, next (*refractory*)=*activity*, next(*activity*)= *firing* forces the transition to the subsequent cellular stage, and $\xi > 1$.
(c) If a FRA cell receives a stimulus then

$$\phi(t+1) = F_1, \qquad \text{if} \;\; \phi(t) = A_l \;\; \text{with} \;\; l = 1, \ldots, a, \tag{2}$$

$$\phi(t+1) = R_{\max\{1, g(l)\}} \qquad \text{if} \;\; \phi(t) = R_l \;\; \text{with} \;\; l = 1, \ldots, r, \tag{3}$$

$$\text{where} \;\; g(l) = \lfloor l \backslash 2 \rfloor$$

The rule (1) is probabilistic. It allows to shorten duration of each stage. But when ξ is large enough then the dynamics becomes deterministic. The rules (1) and (2) together are adaptation of rules used in models of excitable medium [9, 11, 10]. The rule (3) was considered in simple models of two interacting cells only, and, up to our knowledge, it has not been investigated in the network systems.

2.2 The Tissue Model

Physiology of Pacemaker Tissue. The sinus node tissue is flat without any fixed structure. Its contents is usually described as heterogeneous populations of small myocytes [4–8]. The nodal cells form clusters and bundles surrounded by abundant collagen. The node border is a relatively discrete boundary seen between the margins of the node and the adjacent atrial tissues. The transmission of action potentials from cell to cell occurs via large-conductance ion channels, closely packed in large arrays named gap junctions.

Assumptions. Following [11] we assume that the pacemaker tissue is well approximated by a square lattice with open boundary conditions. Each vertex is occupied by a FRA-cell, but only some of lattice neighboring cellular connections are established for inter-cellular interactions. Additionally, we inject heterogeneity to the network by local and intentional wrinkling of inter-cellular connections. The procedure of wrinkling is based on Watts-Strogatz [17] rewiring rule. The intentionality of wrinkling is realized by preferential unlinking from the rare connected neighbors. The locality means that only cells from the close neighborhood can be linked instead. The network of interactions does not evolve. Details of the wrinkling algorithm are given in [18]. Moreover, we assume that cells in *firing* stage are the only source of stimuli to nearest neighbors.

The Model of Network Interactions

(A) A FRA-network of density d consists of $N = L \times L$ FRA-cells located in vertices of square lattice, where any two cells of Moore neighborhood are connected to interact with probability d. The boundary conditions of a lattice are open.

(B) Let a be a FRA-cell and $\mathcal{N}(a)$ be the set of cells interacting with cell a. Let $b \in \mathcal{N}(a)$. For a given $p \in [0, 1]$, probability p_{break} to unlink cell b from the cell a is as follows

$$p_{break} = \frac{p}{\deg(b)}$$

where $\deg(b) = \text{card}\, \mathcal{N}(b)$ is the vertex degree of cell b. A randomly chosen cell $b' \in \mathcal{N}(b)$ is linked to cell a in place of cell b. So, finally $b' \in \mathcal{N}(a)$. The procedure is repeated J Monte Carlo time steps.

Unlinking from a leaf is forbidden. In total, the probability for rewiring of each link is $p * J$. Let us recall that Moore neighborhood on a square lattice comprises the eight cells surrounding the central cell.

2.3 The Control System

The Physiology of the Cardiac Heart Contraction Control. Depolarization of the sinus node cells results in the heart contractions about 100 times per minute. This high rate is constantly modified by the activity of sympathetic and parasympathetic nerve fibers. Parasympathetic activation basically decreases the pacemaker rate by decreasing i^f current. The activation of the sympathetic part of the autonomic regulation acts contrary.

Assumptions. We assume that autonomic regulation acts tonically what reveals in the sensitivity of a FRA-cell to interact with its neighbors.

The Model

Let $N(a, t) = \text{card}\, \{a' \in \mathcal{N}(a) | \phi_{a'}(t) = F_i, i = 1, ..., f\}$ be number of cells interacting with a which at t are in *firing* stage.

Then for a given $F = 0, 1, ...$ and $R = 0, 1, ..$
If $N(a, t) > F$ then rule (2) applies.
If $N(a, t) > R$ then rule (3) applies.

So, F is the sensitivity threshold for interaction of cell a in *activity* stage, and R is the sensitivity threshold for interaction of cell a in *refractory* stage.

3 Results

3.1 Kuramoto Order Parameters to Quantify Collective States

If there is some variation among N interacting oscillators, namely, when an oscillator is isolated then oscillates with own intrinsic frequency, then macroscopic synchronization means that the quantity:

$$\mathcal{K}_f = \frac{M}{N}, \tag{4}$$

has non-zero value. Here M is the size of the largest group of oscillators that attain the same mean frequency. This parameter of synchrony perfectly fits to neuronal interactions. However, in the case of short-range and pulse-like interactions, the more accurate measure of the level of synchrony in a collections of N phase oscillators $\phi_l(t)$ is given by the following quantity:

$$\mathcal{K}_\phi = \frac{1}{N} \left| \sum_{l=1}^{N} e^{i\phi_l} \right|, \tag{5}$$

If all oscillators have the same phase then $\mathcal{K}_\phi = 1$. If phases are scattered at random then $\mathcal{K}_\phi$ is close to zero. Hence, this order parameter quantifies the degree of phase synchronization, whereas $\mathcal{K}_f$ measures the degree of frequency synchronization. A non-zero $\mathcal{K}_\phi$ implies a non-zero $\mathcal{K}_f$, but the opposite is not true.

It turns out [13] that if FRA-network is homogeneous (no wrinkling) and FRA-cell dynamics is deterministic ($\xi >> 1$) then system, evolving under rules (1) and (2) only, is led to states with the perfect adjustment of frequency (hence, $\mathcal{K}_f = 1$) and with the fixed arrangement of cellular phases. The phases of neighboring cells differ by ± 1. Such organization of phases denotes emergence of spiral-wave patterns. The stationary state oscillates either with the natural cellular period $T = f + r + a$ or with the shortest possible: $T^* = f + r + 1$. Rarely, a period occurs which length is between T^* and T. In all these cases, the order parameter $\mathcal{K}_\phi$ is significantly greater than 0 and its value depends on periodicity of the wave. But the spiral patterns are observed in the real cardiac tissue only in the pathological cases [6–8].

Entering rule (3) results in that any two neighboring cells always gain the phase difference equal to zero, asymptotically [14]. It means that in the network of FRA-cells we observe the perfect phase synchronization with $\mathcal{K}_\phi = 1$.

This state is called *marching cells*. Moreover at certain model parameters waves collapsing inward occur. Again, all such states in the real sinus node tissue are a manifestation of pathological changes.

Notice that because of (3) the periods of states with stationary wave-patterns can be elongated. For example, at wave phase adjustment in a line of FRA-cells, the following pattern is stable:

$$\begin{array}{rcccccc} t-1: & F_{f-2} & F_{f-1} & F_f & R_1 & R_1 & R_2 \\ t: & F_{f-1} & F_f & R_1 & R_1 & R_2 & R_3 \\ t+1: & F_f & R_1 & R_1 & R_2 & R_2 & R_4 \end{array} \tag{6}$$

what means that the period of the state oscillations is greater than a natural cell period by 1.

3.2 Results from Simulations

In Figs 3 – 6 the results are shown in terms of order parameters $\mathcal{K}_f$ and $\mathcal{K}_\phi$ for densities d large enough to observe the collective properties.

From Fig. 3, describing systems with deterministically evolving FRA cells located on homogeneous networks, we see that the solutions are firmly determined. The parameter $\mathcal{K}_f$ equals to 1 in large intervals of densities d and for many values of F and R. This means that all cells oscillate with the same period. Only if $F = 3$ and $R = 0$ the value of $\mathcal{K}_f$ drops down. Furthermore, when d is changing, the switch is observed in the state periodicity from oscillations other than T (shorter than T in case $F = 0, 1$, or longer than T in case $F = 2, 3,$) to the oscillation with T.

States oscillating with period different from T demand permanent entrainment between cellular states. The transitions are observed for densities in $\Delta_c = \{d : 0.5 < d < 0.8\}$. From Fig. 4 we see that there are essential changes in $\mathcal{K}_\phi$ value for densities in Δ_c interval. Outside this interval, if $d > \Delta_c$, then $\mathcal{K}_\phi$ often reaches 1, while in the case of small density the phase synchronization is, in general, small.

Combining the values of order parameters for models with $F = 0$ and $R = 1$ or $R = 2$ with the dominant oscillations presented in Fig. 3, we can give the direct interpretation for $\mathcal{K}_\phi$ values as follows. If a state is a spiral wave with the shortest period T^* then $\mathcal{K}_\phi \approx 0.5$. If a state oscillates with the cellular period T then $\mathcal{K}_f \approx 0.2$. These estimates agree with the rough assessment based on the mean field calculations.

Comparing the listed results to the corresponding properties shown in Fig. 5 we can learn which properties survive inclusion of stochastic dynamics and heterogeneity into the intercellular connections. The rough observation indicates that dependence of dominant oscillation on density d is similar to that observed in the rigid systems. However, now the participation of the dominant period is much smaller. Notice that for all F and R considered by us, $\mathcal{K}_f < 0.3$. Moreover, from Fig. 4 we see that $\mathcal{K}_\phi$ never attains 1. But, on the other hand, $\mathcal{K}_\phi$ is also significantly distinct from 0. Hence the high level of phase synchronization is

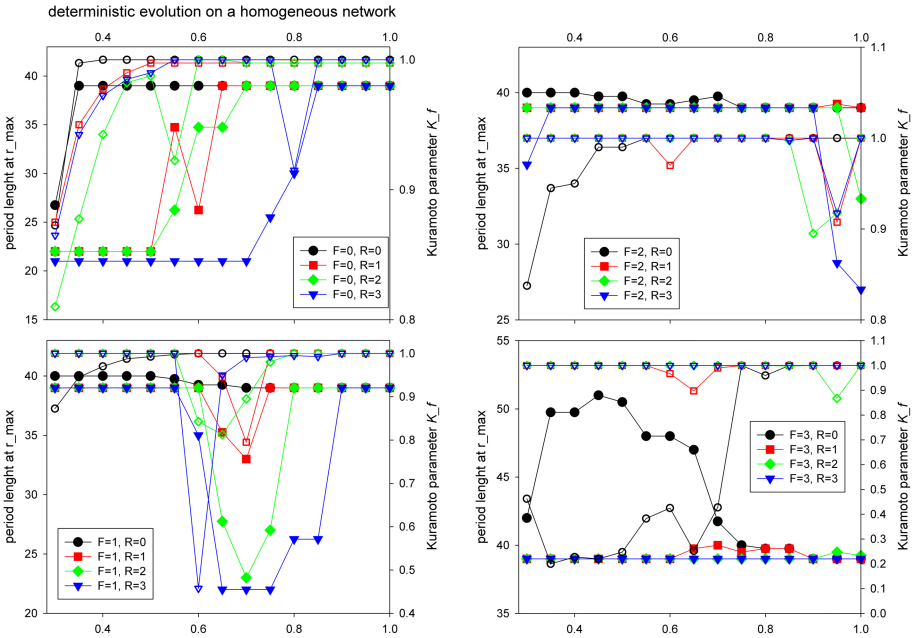

Fig. 3. Kuramoto order parameter $\mathcal{K}_f$ (empty marks) and the most frequent period (filled marks) for different densities d, and for different sensitivity F and R in stationary states obtained from system performing deterministic dynamics on not wrinkled networks. *Simulation condition:* the lattice size $N = 10^4$ and $f = 9, r = 11, a = 19$; plots represent mean values from 10^4 time steps and 50 independent simulation experiments. The first 10^4 time steps were skipped to let the system stabilize.

achieved in stationary states. The phase synchronization emerges due to the fact that distributions of periods are concentrated around the dominant period. In Fig. 6 we show distributions of period lengths for some model parameters. We see that in most cases the distribution is a modal one. However, also bimodal distributions appear for densities $d \in \Delta_c$.

It is worth noting, that for the model parameters $F = 1, R = 2, 3$ and $d \in (0.6, 0.7) \subset \Delta_c$, independently of the cellular dynamics (deterministic or stochastic) and of network structure (homogeneous or intentionally wrinkled), the value of $\mathcal{K}_\phi$ is the same. So the state of the system is firmly kept with the common oscillations though the value of the period can change from the shortest oscillations to the natural cellular oscillations. Since the natural systems often work at the edge of criticality then we hypothesize that these FRA-systems correspond to the natural pacemaker in the best way. The strong support for our hypothesis comes from the fact that Δ_c falls into densities which are observed in the real sinus node tissue [4].

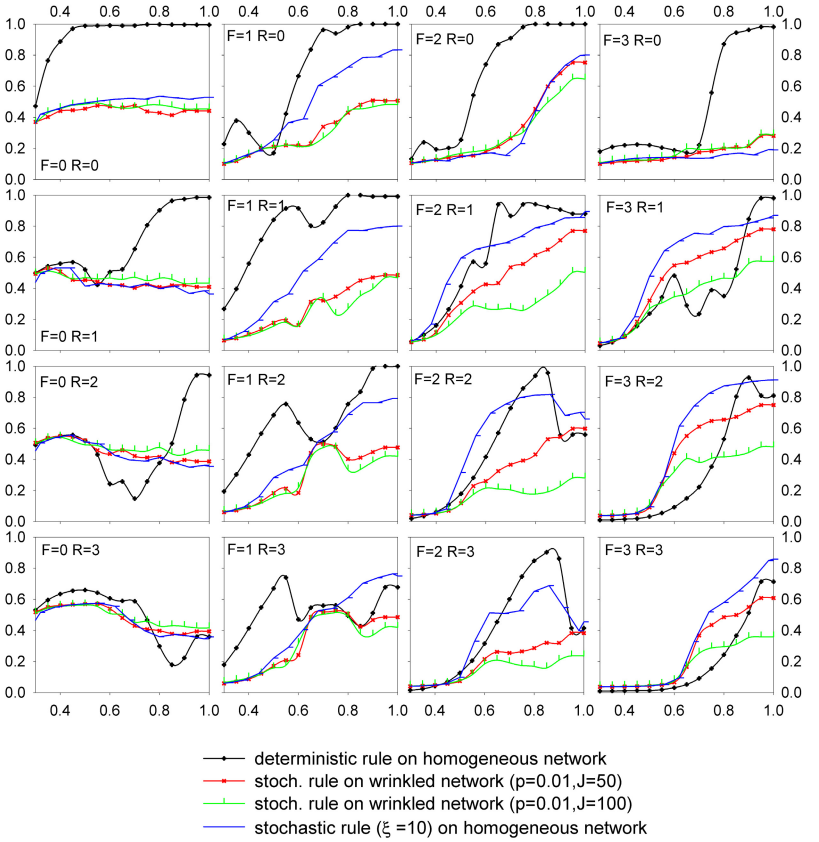

Fig. 4. Kuramoto order parameter $\mathcal{K}_\phi$ of stationary states for different density of stochastic network connections, sensitivity F and R of interactions, cellular dynamics (deterministic versus stochastic with $\xi = 10$), and network structure (homogeneous versus heterogeneous due to wrinkling). Simulations conditions are described in Fig.3

4 Discussion

Cardiac cell cultures are becoming important experimental systems of minimal complexity that capture many of the salient features of myocardial tissue function and are simple enough that the tissue parameters can be controlled systematically [11, 12]. Between the two pathological network states of strongly entrained spiral waves and marching cells which are observed in both computer and biological tissue models, there are many states with physiologically justified properties. Hence, by discrete modeling we provide tools to formalize the biological observations. Here, especially Kuramoto order parameters $\mathcal{K}_f$, $\mathcal{K}_\phi$ justified their ability to qualify and quantify the collective features in the multi parameter model. However, the next challenge is to send the model results back to physiologists, so they can use them iteratively as the input in their further experiments.

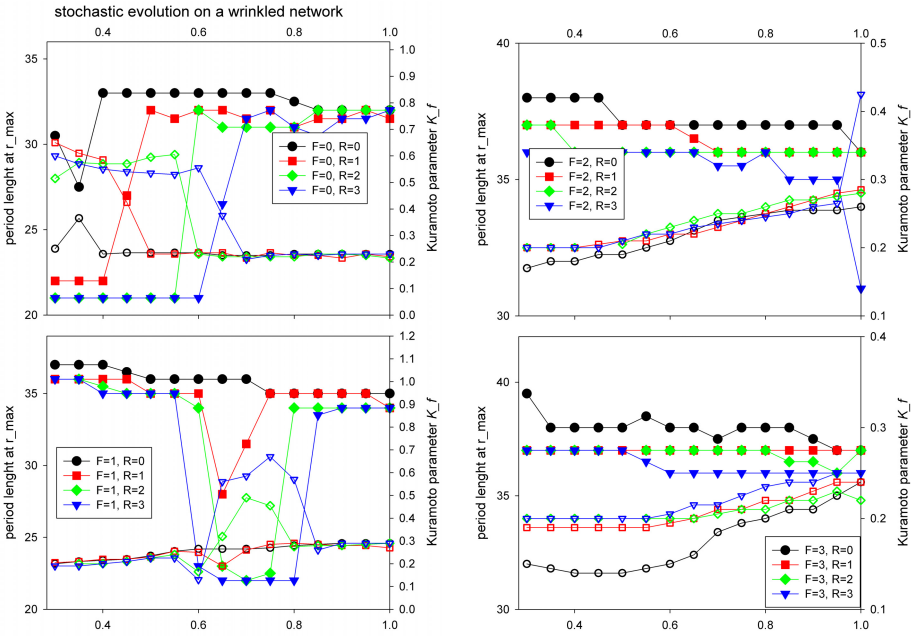

Fig. 5. Kuramoto order parameter $\mathcal{K}_f$ (empty marks) and the most frequent period (filled marks) for different densities d, and for different sensitivity F and R in stationary states obtained from systems driven by stochastic dynamics with $\xi = 10$, and on wrinkled networks when $p = 0.01, J = 50$. Simulations conditions are described in Fig.3.

Therefore, when closing we concentrate on clarification if the model results are able to reveal some changes in the sinus node with age.

The function of the sinus node declines with age, leading to a condition called sick sinus syndrome [5, 8, 21]. Aging causes a decrease in the overall intrinsic heart rate, and an increase in the nodal conduction time. These changes are preceded by a period of tissue remodeling — significant structural changes in the intracellular matrix caused by increase of the collagen tissue. The collagen deposition can be thought as limiting the plasticity of the network connections what translates to FRA system as less wrinkled underlying networks of interactions. In consequence, if $F = 1$, then tendency to the solution with marching cells appears, see blue lines in Fig. 4. Moreover, together with collagen increase, the density d could be though as decreased, what leads, according to our results, to states where strongly entrained spirals emerge.

Age dependent alternations in ion channels (by perturbations in expression and/or function of genes) influence both the intrinsic cellular cycle and sensitivity of a cell for interactions. For example, there is observed a decrease in potasium $\mathbf{i_K}$ current with aging in the rat sinus node which could be linked to the observed increase in action potential duration with aging [22]. Such properties can be easily coded in FRA systems. By varying with durations of particular stages of FRA-cell cycle one reconstructs effects of changes in particular parts

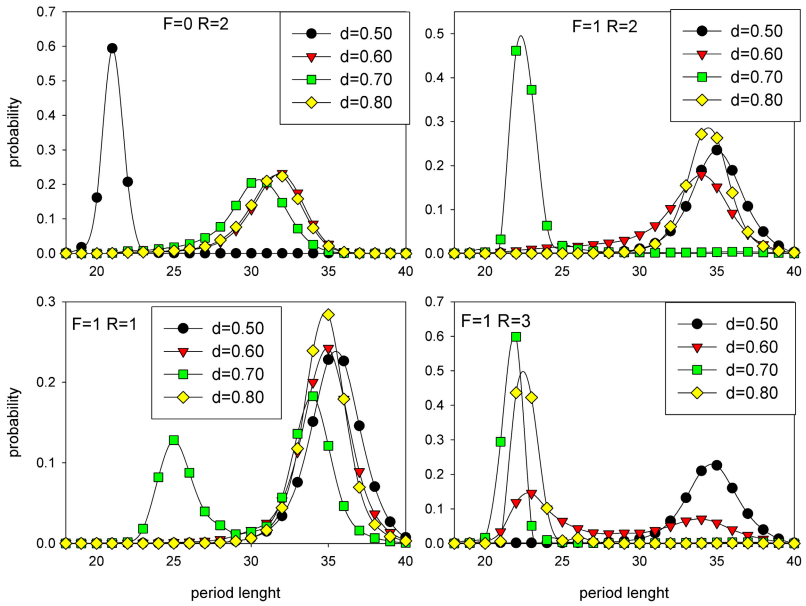

Fig. 6. Distribution of periods observed in some stationary state at given model parameters: stochastic dynamics, $\xi = 10$, wrinkling at $p = 0.01, J = 0.01$. Other parameters are the same as described under Fig.3.

of the intrinsic cell period. Modifications in values of F and R parameters allow to reveal effects of the impairment of sensitivity. It appears that if F changes from 1 to 2 or 3 then only heterogeneity in the network connection which is strong enough, protects against appearance of entrained spirals. If additionally R decreases then desynchronization occurs - there is no source of the leading oscillation independently of the level of heterogeneity.

References

1. Stumpf, M., Balding, D.J., Gorolami, M.: Handbook of Statistical Systems Biology. Wiley (2011)
2. Jalife, J., Delmar, M., Davidenko, J., Anumonwo, J., Kalifa, J.: Basic Cardiac Electrophysiology for the Clinician. Wiley-Blackwell (2009)
3. Klabunde, R.E.: Cardiovascular Physiology Concepts. accesible via, `http://www.cvphysiology.com/Arrhythmias/A005.html`
4. Saffitz, J.E., Lerner, D.L., Yamada, K.A.: Gap Junctions Distribution and regulation in the Heart. In: Zipes, D.P., Jalive, J. (eds.) Cardiac Elecrophysiology. From Cell to Bedside, pp. 181–191. Saunders Co., Philadelphia (2004)
5. Dobrzynski, H., Boyett, M.R., Anderson, R.H.: New Insights Into Pacemaker Activity: Promoting Understanding of Sick Sinus. Circulation 115, 1921 (2007)
6. Mangoni, M.E., Nargeot, J.: Genesis and Regulation of the Heart Automaticity. Physiol. Rev. 89, 919 (2008)

7. Aslanidi, O.V., Boyett, M.R., Dobrzynski, H., Zhang, H.: Mechanisms of transition from normal to reentrant electrical activity in a model of rabbit atrial tissue: interaction of tissue heterogeneity and anisotropy. Biophysical J. 96, 7989 (2009)
8. Boyett, M.R.: 'And the beat goes on' The cardiac conduction system: the wiring system of the heart. Experimental Physiol. 94, 1035 (2009)
9. Greenberg, J.M., Hastings, S.P.: Spatial patterns for discrete models of diffusion in excitable media. SIAM J. Appl. Math. 34, 515 (1978)
10. Berry, H., Fatés, N.: Robustness of the critical behaviour in the stochastic Greenberg-Hastings cellular automaton model. IJUC 7, 65 (2011)
11. Bub, G., Shrier, A., Glass, L.: Global Organization of Dynamics in Oscillatory Heterogeneous Excitable Media. Phys. Rev. Lett. 94, 028105 (2005)
12. Chang, M.G., Zhang, Y., Chang, C.Y., Xu, L., Emokpae, R., Tung, L., Marban, E., Abraham, M.R.: Spiral waves and reentry dynamics in an in vitro model of the healed infarct border. Circ. Res. 105, 1062 (2009)
13. Makowiec, D.: Modeling the sinoatrial node by cellular automata with irregular topology. Int. J. Mod. Phys. C 21, 107 (2010)
14. Makowiec, D.: Phase-sensitive cellular automata on stochastic network as a model for cardiac pacemaker rhythmicity. Acta Phys. Pol. B Proc. Supp. 5, 85 (2012)
15. Michaels, D.C., Matyas, E.P., Jalife, J.: Dynamic interactions and mutual synchronization of sinoatrial node pacemaker cells. Circ. Res. 58, 706 (1986)
16. Anumonvo, J.M., Delmar, M., Vinet, A., Michaels, D.C., Jalife, J.: Phase resetting and entrainment of pacemaker activity in single sinus nodal cells. Circ. Res. 68, 1138 (1991)
17. Watts, D.J., Strogatz, S.H.: Collective dynamics of 'small-world' networks. Nature 393, 409 (1998)
18. Makowiec, D.: Evolving network - simulation study. From a regular lattice to scale free network. EPJ B 48, 547 (2005)
19. Kuramoto, Y.: Chemical Oscillations, Waves and Turbulence. Springer, Berlin (1984)
20. Acebron, J.A., Bonilla, L.L., Vicente, C.J.P., Ritort, F., Spigler, R.: The Kuramoto model: A simple paradigm for synchronization phenomena. Rev. Mod. Phys. 77, 137 (2005)
21. Rose, A.: Keeping the clock ticking as we age: changes in sinoatrial node gene expression and function in the aging heart. Exp. Physiol. 96, 1114 (2011)
22. Alings, A.M., Bouman, L.M.: Electrophysiology of the ageing rabbit and cat sinoatrial node-a comparative study. Eur. Heart J. 14(9), 1278 (1993)